*Acta Cryst.* (1995). D**51**, 220–231

# Crystallographic Analysis of Phe→Leu Substitution in the Hydrophobic Core of Barnase

BY YU WAI CHEN, ALAN R. FERSHT AND KIM HENRICK*

*Centre for Protein Engineering, Medical Research Council Centre, Hills Road, Cambridge CB2 2QH, England*

(*Received* 22 *April* 1994; *accepted* 29 *July* 1994)

## Abstract

The crystal structure of a barnase mutant, Phe→Leu7 has been determined to 2.2 Å resolution. No structural rearrangement is observed near the mutated residue. The F7L mutation is highly destabilizing and this is caused by the loss of extensive van der Waals contacts that wild-type Phe7 made with its neighbouring residues, and the exposure of a large hydrophobic pocket on the surface of the protein. The side-chain conformations of the mutated Leu7 residue have torsion angles $\chi_1$ ranging from −138° to −168° and $\chi_2$ ranging from +16° to +70°, for the three molecules in the asymmetric unit. These angles do not agree with the most frequently observed conformations in the protein side-chain rotamer library [Ponder & Richards (1987). *J. Mol. Biol.* **193**, 775–791]. However, when compared to a more recent 'backbone-dependent' rotamer library [Dunbrack & Karplus (1993). *J. Mol. Biol.* **230**, 543–574], the side-chain conformation of Leu7 agrees well with that of the most frequently observed rotamers. The side-chain conformation of Leu7 was found to be dictated by two factors: it has the lowest conformational energy and it buries the most hydrophobic surface area.

## Introduction

Barnase is a small (110 residues) ribonuclease enzyme (Mauguen *et al.*, 1982; Hill, 1986; Cameron, 1992) of *Bacillus amyloliquefaciens* which has been used extensively as a model system in protein-folding studies. A systematic programme of site-directed mutations has being undertaken to investigate the effect of specific interactions on the stability of proteins. X-ray crystallography has been employed as a complementary tool in aiding the interpretation of various protein-engineering results.

In an earlier attempt to quantify the contribution of hydrophobic interactions to protein stability, three barnase mutants were designed to generate cavities of various sizes in the hydrophobic core (Kellis, Nyberg, Sali & Fersht, 1988). The initial idea of preparing the Phe→Leu7 (F7L) mutant was, to create a hole having a size approximating three $CH_2$ groups in the hydrophobic core, to probe the loss of stabilization energy in relation to the size of the cavity. From previous denaturation experiments, it has been established that this mutant is very much destabilized relative to the wild type (Kellis, Nyberg, Sali & Fersht, 1988).

In wild-type barnase, residue Phe7 is located near the N-terminal end of the major α-helix (α1), and at the edge of the major hydrophobic core. The side chain of this residue is pointing into the centre of the core, packing against the side chains of Ile76, Asp86, Lys98, Thr100 and Ile109 (Fig. 1). This residue is largely buried and has an accessible surface area of 26–30 Å$^2$ [calculated with the program *DSSP* by Kabsch & Sander (1983)]. The side-chain atoms of Phe7 form extensive van der Waals contacts with many hydrophobic side chains in the core (Table 1 and Fig. 2). Most of these contacts were expected to be removed or altered on mutation.

Here we report the high-resolution crystal structure of this cavity-creating mutant. By solving its crystal structure, we would be able to correlate the loss in stabilization energy to the removed interactions of interest. The mutation of a phenylalanine into a leucine residue has been generally assumed to be conservative and non-disruptive despite the fact that there is a change in configuration of $C^\gamma$ from $sp^2$ to $sp^3$. By examining the side-chain conformation of the mutated leucine residue in high resolution, it will be possible to tell how true this assumption stands. The crystal structure will also reveal whether there are any solvent molecules filling in the large hydrophobic cavity created by mutation and whether the solvation of the protein at the mutation site has changed.

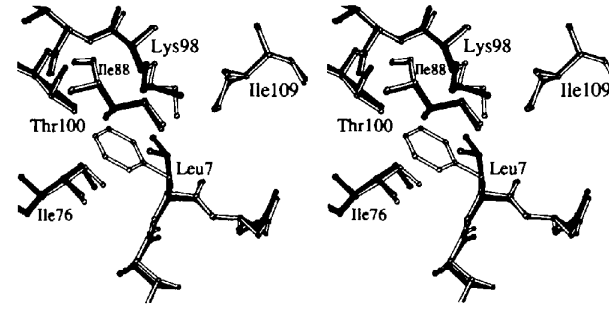


Fig. 1. The comparison of residue 7 of wild-type barnase and of the F7L mutant. The wild-type structure at pH 7.5 contains a $Zn^{2+}$ ion (Hill, 1986) was compared to the F7L structure, which also contains a $Zn^{2+}$ ion. Filled bonds are for the mutant structure, hollow bonds are for the wild type. This figure is generated with *MOLSCRIPT* (Kraulis, 1991).

* Present address: National Institute for Medical Research, The Ridgeway, Mill Hill, London NW7 1AA, England.

Table 1. *The interactions made by the side chain of residue Phe7 in the wild-type structure that are affected by mutation*

| Residue in contact | Atom in contact | Distance (Å) | | |
|---|---|---|---|---|
| | | *A* chain | *B* chain | *C* chain |
| Ile76 | $C^{\beta}$ | 3.8 | 4.0 | 3.8 |
| | $C^{\gamma 1}$ | 3.6 | 3.8 | 3.6 |
| | $C^{\gamma 2}$ | 3.7 | 3.9 | 3.6 |
| Asp86 | $C^{\beta}$ | 4.0 | 3.8 | 3.8 |
| Arg87 | C | 4.0 | 4.1 | 3.9 |
| | O | 3.4 | 3.6 | 3.5 |
| Lys98 | $C^{\beta}$ | 3.7 | 3.4 | 3.6 |
| | $C^{\delta}$ | 3.7 | 4.0 | 4.0 |
| | $N^{\zeta}$ | 3.9 | 4.4 | 3.6 |
| Thr99 | O | 4.0 | 3.9 | 4.0 |
| Thr100 | $C^{\gamma 2}$ | 4.2 | 3.7 | 4.0 |

Table 2. *Crystallographic data for the barnase F7L mutant*

| Data collection | Film |
|---|---|
| Cell dimensions* | |
| $a = b$ (Å) | 58.7 |
| $c$ (Å) | 82.0 |
| Resolution (Å) | 6- 2.2 |
| Total No. of reflections | 26504 |
| No. of independent reflections | 15097 |
| Completeness of data (%)† | 94.0 (77.1) |
| Multiplicity of data (%)† | 1.5 (1.4) |
| $R_{merge}$ (%)† | 8.0 (5.3) |
| $R$ factor between $F'_{obs}$ of F7L and that of the wild type (%) | 52 |

* Cell dimensions for wild-type barnase (pH 7.5) are: $a = b = 59.0$, $c = 81.6$ Å, at 2.0 Å resolution.

† The values in parentheses are for the highest resolution bin (2.26–2.20 Å).

## Experimental methods

*Crystallization and data collection*

Barnase mutagenesis, expression and purification were performed as described previously (Kellis, Nyberg, Sali & Fersht, 1988) with the modification that the cells are grown at 303 K because the F7L mutant enzyme is very unstable. Crystallization of barnase mutants was based on a procedure of Dr Hartley (Bethesda, USA) using the hanging-drop method (Chen, Fersht & Henrick, 1993). The crystals are hexagonal rod-like which are the same as those of the wild type (Mauguen *et al.*, 1982), belonging to the space group $P3_2$, with three molecules in the asymmetric unit.

A single F7L crystal measuring approximately 0.2 × 0.2 × 0.6 mm was used to collect a complete data set to 2.2 Å on oscillation films at 278 K at the SRS station PX7.2 ($\lambda$ = 1.488 Å) at Daresbury, England. A total of 32 packs were collected using a rotation angle of 2.3° per exposure. Reflection spots were found to be split from pack 20 onwards and these packs were not processed. Therefore, the effective angular coverage was 46.0°. Films were digitized on an Optronix photoscanner using a 50 mm raster step size.

All data processing employed the *CCP*4 program suite (Collaborative Computational Project, Number 4, 1994; Buckle, Henrick & Fersht, 1993; Chen, Fersht & Henrick, 1993). Data-processing statistics are summarized in Table 2.

*Structure solution and refinement*

The F7L structure could not be solved directly by refinement starting from wild-type coordinates, because of non-isomorphism of wild-type and mutant data (Table 2), and the molecular-replacement method was employed. This non-isomorphism presumably arises from the slight internal rotation of individual protein chain within the asymmetric unit and is a common feature of barnase mutant crystals (Buckle, Henrick & Fersht, 1993; Chen, Fersht & Henrick, 1993; Chen, 1994). The method of applying molecular replacement, using the *CCP*4 suite of programs, to solve barnase mutants has been published previously (Chen, Fersht & Henrick, 1993). The cross-rotation function search found three solutions almost equal in magnitude at 6.0$\sigma$ ($\alpha$ = 23, $\beta$ = 53, $\gamma$ = 303°), 5.8$\sigma$ ($\alpha$ = 60, $\beta$ = 131, $\gamma$ = 127°) and 5.5$\sigma$ ($\alpha$ = 45, $\beta$ = 131, $\gamma$ = 127°), and the next highest peak was at 4.2$\sigma$. These three peaks correspond to the three molecules in the asymmetric unit. Translation search with *TFSGEN* found three solutions approximately equal in height (11.2$\sigma$, 11.1$\sigma$ and 10.9$\sigma$, next highest peak at 3.6$\sigma$) and related by symmetry. The highest peak (fractional coordinates: $x = 0.955$, $y = 0.901$, $z$ set to 0.0) was picked and used for further searches. The first run of *TFPART* identified a single highest peak (17.0$\sigma$, next highest peak at 4.5$\sigma$) at fractional coordinates $x = 0.239$, $y = 0.489$, $z = 0.824$. *TFPART* second run also found one highest peak (23.6$\sigma$, next highest peak at 4.7$\sigma$) at fractional coordinates $x = 0.562$, $y = 0.311$, $z = 0.040$. These three translation-function solutions were applied to the three corresponding rotation-search solutions and this became the complete molecular-replacement solution of the three molecules in the asymmetric unit. The solution was displayed on a graphics station and the packing between chains was good. The three molecules in the asymmetric unit of the mutant structure are in roughly the same positions as those of the wild-type structure.

At this stage, the three solutions were assigned chain names of *A*, *B* and *C*, according to the wild-type nomenclature. This was done by superposing each of the three molecular-replacement solution chains onto the three wild-type chains in turn. With the aid of the molecular graphics program *O* (Jones, Zou, Cowan & Kjeldgaard, 1991), only one superposition was found to have all the symmetry-related neighbours agreeing, and the chains could then be uniquely identified.

The molecular-replacement solution model was then subjected to rigid-body refinement in *X-PLOR* (Brünger, Kuriyan & Karplus, 1987), with each barnase F7L chain treated as a single group. The *R* factor dropped from 42 to 30%. Following this, energy minimization

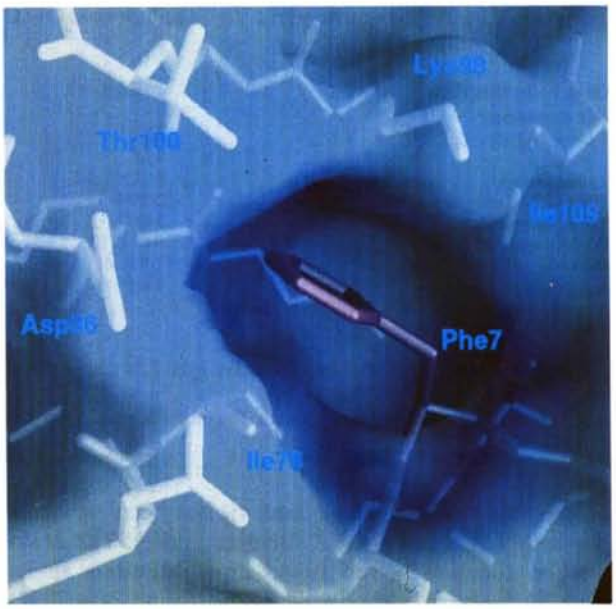


Fig. 2. The side chain of wild-type barnase residue Phe7 (magenta) and the molecular surface of its neighbouring residues (white) in van der Waals contact which are affected by mutation. The molecular surface was calculated with a probe radius of 1.70 Å. A second molecular surface was calculated for residue Phe7 alone. The surface shown here is colour coded with the deepest blue representing the closest contact between the two surfaces. Distances longer than 4 Å are coloured in white. This picture, Fig. 3 and Fig. 8 were created with the program *GRASP* (Nicholls, 1992).

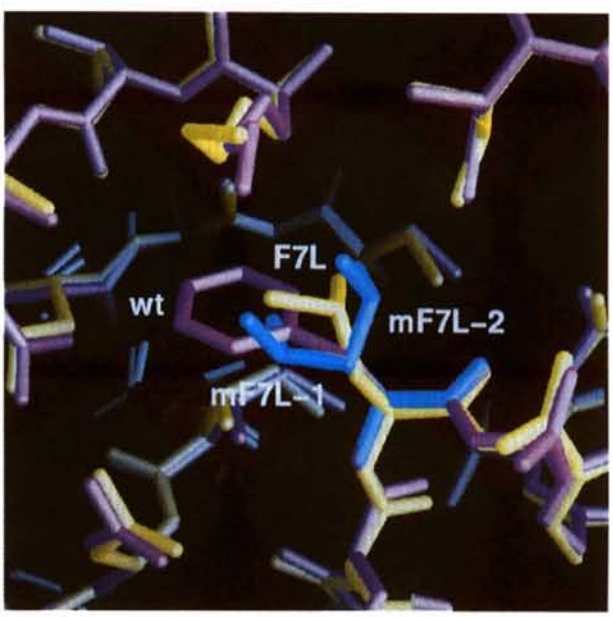


Fig. 3. Comparison of the side-chain conformations of the mutated residue Leu7 (yellow) in the F7L crystal structure, and that in the two 'modelled F7L-rotamers' (mF7L-1 and mF7L-2, cyan) representing the two most frequently observed rotamers in the library of Ponder & Richards (1987), respectively. The wild-type residue Phe7 is also shown in magenta.

Table 3. *Summary of least-squares refinement statistics for the barnase F7L mutant*

| | | |
|---|---|---|
| Crystallographic $R$ factor (%)* | | |
| For all data in the resolution range 10–2.2 Å | | 18.3 (15001) |
| For all data in the resolution range 6–2.2 Å | | 17.4 (14480) |
| For data with $F > 2\sigma(F)$ in the resolution range 6–2.2 Å | | 16.8 (13877) |
| | Target $\sigma$ | Final model |
| R.m.s. deviations from ideal distances (Å) | | |
| Bond distance (1–2 neighbour) | 0.020 | 0.020 |
| Angle distance (1–3 neighbour) | 0.040 | 0.058 |
| Planar distance (1–4 neighbour) | 0.050 | 0.058 |
| R.m.s. deviation from ideal planarity (Å) | 0.020 | 0.017 |
| R.m.s. deviation from ideal chiral volume (Å$^3$) | 0.120 | 0.159 |
| R.m.s. deviations from ideal non-bonded contact restraints (Å) | | |
| Single-torsion contact | 0.200 | 0.181 |
| Multiple-torsion contact | 0.200 | 0.185 |
| Possible hydrogen bond ($X \cdots Y$) | 0.200 | 0.199 |
| R.m.s. deviations from ideal conformational torsion angles (°) | | |
| Planar (0°, 180°) | 3.00 | 2.69 |
| Staggered (±60°, 180°) | 20.00 | 18.94 |
| Orthonormal (±90°) | 15.00 | 16.14 |
| R.m.s. deviations from ideal thermal factor (Å$^2$) | | |
| Main-chain bond | 1.50 | 1.45 |
| Main-chain angle | 2.00 | 2.21 |
| Side-chain bond | 2.00 | 2.51 |
| Side-chain angle | 3.00 | 3.55 |
| No. of protein atoms† | | 2526 (16.6) |
| No. of $Zn^{2+}$ ions per asymmetric unit†‡ | | 1 (19.9) |
| No. of solvent molecules† | | 226 (24.3) |

*Crystallographic $R$ factor is defined as, $R = (\Sigma||F_o| - |F_c||)/\Sigma|F_o|$. The number of reflections included are in parentheses.

† The number of protein atoms, $Zn^{2+}$ ions and solvent molecules are listed with their corresponding mean $B$ factors (Å$^2$) in parentheses.

‡ The $Zn^{2+}$ ion in F7L is found in the same Zn site (Hill, 1986) of the wild-type pH 7.5 structure (r.m.s. deviation = 0.16 Å).

using molecular dynamics was performed to allow for some initial large atomic movements, using the *X-PLOR* simulated-annealing (slow cool) protocol. The $R$ factor of the model dropped to 28%. From then on, the structure model was refined with successive cycles consisting of manual rebuilding using the program, *O* (Jones & Kjeldgaard, 1993), followed by restrained least-squares refinement using *PROLSQ* (Collaborative Computational Project, Number 4, 1994; Hendrickson, 1985). The refinement restraint parameters and the statistics of the final model were tabulated in Table 3.

### *Generation of modelled F7L mutants*

In order to study the side-chain conformation of the mutated Leu7 side chain, two 'modelled F7L-mutant' structures were generated. These were created first with the 'Mutate_Replace' and subsequently the 'Lego_Side_Chain' commands in *O*, starting from the wild-type crystal structure at pH 7.5, including solvent molecules. The side chains of Phe7 for all three chains were replaced with the leucine rotamers taken from the rotamer library (Ponder & Richards, 1987) implemented in *O* (Fig. 3). 'Model-F7L-1' corresponds to the most

frequently observed rotamer: $\chi_1 = -60°$, $\chi_2 = 180°$; while 'model-F7L-2' corresponds to the second-most frequently observed rotamer: $\chi_1 = 180°$, $\chi_2 = +60°$. These two modelled F7L structures were then subjected to 40 steps of conjugate gradient minimization in *X-PLOR*. During minimization, several constraints were applied: (1) interactions were constrained to include only atoms within a 10 Å sphere from Leu7 of the respective chain; (2) all main-chain atomic positions were fixed; (3) the dihedral angle $\chi_1$ of Leu7 (all chains) was constrained so that the rotamer conformations were preserved in the respective modelled F7L structures. This minimization procedure simulates the relaxation of the protein to remove bad local contacts, while keeping the backbone unchanged.

*Conformational energy calculations*

To investigate the variation in conformational energy with the torsion angle $\chi_1$ of residue Leu7 in the F7L crystal structure, 36 F7L '$\chi_1$-rotamer' structures were generated with $\chi_1$ sampling every 10° of rotation. These structures were created with the 'Tor_Residue' command in *O*, starting from the F7L crystal structure, including water molecules. All these structures were energy minimized as described under *Generation of modelled F7L mutants* to remove poor contacts before energy calculations. For each of these 36 structures, the total energy (bond, angle, dihedral, improper, van der Waals and electrostatic) were calculated between Leu7 and all neighbouring atoms within a 10 Å sphere. These energies were also calculated for the two modelled mutant structures. All calculations were performed with *X-PLOR*.

*Molecular surface area calculations*

The molecular surface area buried by residue Leu7 in various structures were calculated with the program *MS* (Connolly, 1983), using a probe radius of 1.35 Å and the following procedure. First, the molecular surface area of neighbouring residues excluding Leu7 was calculated. Secondly, the molecular surface area of Leu7 alone was calculated and added to the first item. This sum is the total molecular surface area before burial. Thirdly, the observed molecular surface area of all neighbouring

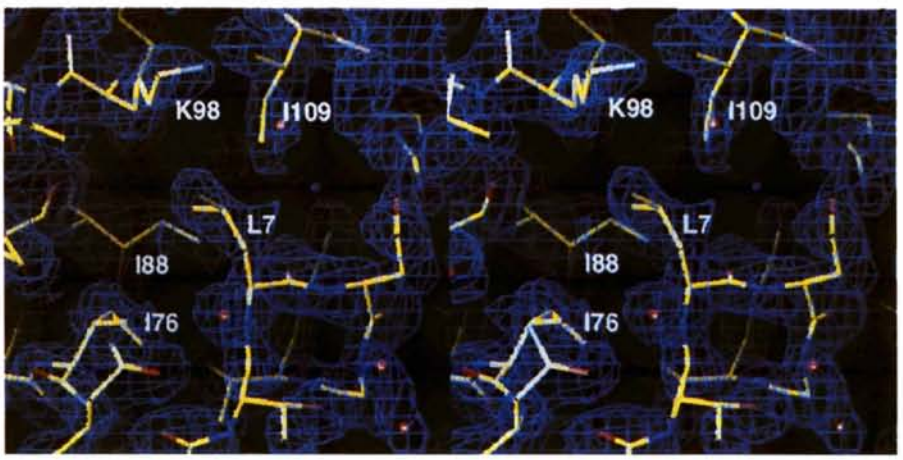


Fig. 4. Stereo pictures showing $3F_o - 2F_c$ electron density contoured at $1.3\sigma$ for the surroundings of residue Leu7 in the F7L mutant.

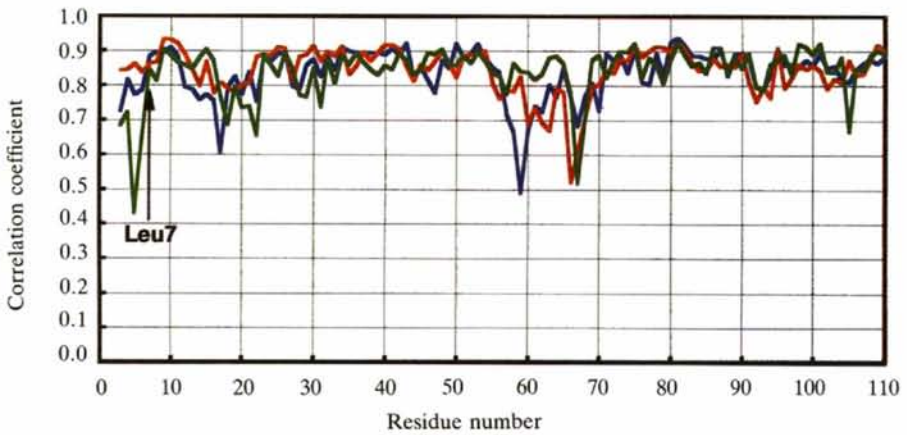


Fig. 5. Real-space correlation coefficient per residue for all atoms (Jones, Zou, Cowan & Kjeldgaard, 1991; Jones & Kjeldgaard, 1993) calculated for the F7L mutant chains *A* (blue), *B* (red) and *C* (green). A value of 1.0 indicates a perfect fit of the structure model and the electron density. The residues in the guanine-binding loop (residues 58–60 and 65–69) are poorly defined.

residues including Leu7 was calculated. The difference between the total area to be buried and the observed molecular surface area is the amount of surface area buried by the residue Leu7.

## Results

*Quality of structure models*

The refinement was straightforward and no major rebuilding was necessary. The final crystallographic *R* factor is 17.4% (Table 3) and the error in the coordinates was estimated by a Luzzati plot (Luzzati, 1952, not shown) to be 0.21 Å. The electron densities for the mutated residues were well defined (Fig. 4). The real-space correlation coefficient plot (Fig. 5) (Jones, Zou, Cowan & Kjeldgaard, 1991), was included to show the agreement of the model to the electron density per residue. The mutation site of F7L is in proximity to the N terminus. As in the wild-type barnase structure and other barnase mutant structures, this region is in very poor density and the first two or three residues are always disordered. It is possible that this part of the protein lacks intra-molecular hydrogen bonds and therefore takes up a number of alternative conformations in the crystal lattice, making the electron densities around this region difficult to interpret. In the F7L mutant, the N-terminal region is poorly defined up to residue 5 in the *C* chain. When analysing local structural changes, it is important to note that the *C* chain is the least reliable for the F7L mutant whereas in the wild-type structures, the *C* chain is the most ordered. For most analyses, results derived from the *A* and *B* chains agree well while discrepancy is observed in the *C* chain. The residues in the guanine-binding loop (residues 58–60 and residues 65–69) are also poorly defined, presumably because the loop is disordered in the crystal. This is also observed in the wild-type structures and other barnase mutants. The electron density in this region is so poor that a continuous main chain cannot be constructed.

*Overall structure comparison with the wild type*

Within the limit of the coordinate errors, no major conformational changes have been observed (Fig. 1). The r.m.s. difference in the atomic positions for the mutant structure comparing with the wild-type structure is shown in Fig. 6. The average r.m.s. differences among individual mutant chains (~0.6 Å) are slightly higher than that among the wild-type chains (~0.46 Å), and the overall r.m.s. differences between a mutant chain and its corresponding wild-type chain (~0.46 Å). The intra-asymmetric unit r.m.s. differences can be considered as an indication of the barnase molecule, especially its surface residues and the atoms in the flexible loop regions, taking up slightly different alternative conformations during crystallization. In this context, the overall structural change due to mutation, is smaller than the structural changes resulting from crystal packing. Therefore, this Phe→Leu mutation is non-disruptive and the hydrophobic interactions removed are not essential for correct folding.

*Localized structure comparison with the wild type*

To study the localized effect induced by mutation, the individual chain that has the best quality (lowest overall and localized *B* factors and highest overall and localized real-space correlation, Figs. 5 and 7) will be discussed. Unlike the wild-type structures and all other barnase mutant structures, which have the *C* chain best defined (Buckle, Henrick & Fersht, 1993; Chen, Fersht & Henrick, 1993), F7L has the *C* chain defined worst. Chains *A* and *B* are equally good in their overall qualities. The *B* chain was selected for further analysis because it has a better local quality around the site of mutation.

The result of the F7L mutation is the creation of a large hydrophobic depression on the surface of the protein, rather than a cavity (Fig. 8). This 'pocket' is solvent accessible and has an area of approximately 50 $Å^2$. Many of the van der Waals contacts made by the Phe7 in the wild type (Table 1) are removed and some new contacts are made by Leu7 in the mutant (Table 4). The interactions removed include those made with residues Ile76, Asp86, Arg87, Thr99 and Thr100. Residue Leu7 makes two new interactions with $C^{\delta 1}$'s of Ile88 and of Ile109.

Neither the residues that make van der Waals interactions with Phe7 in the wild type (residues Ile76, Asp86, Arg87, Lys98, Thr99 and Thr100) nor the residues that

| | | | | | | |
|---|---|---|---|---|---|---|
| F7L | B | 0.53 | | | | |
| | C | 0.64 | 0.59 | | | |
| | A | 0.45 | — | — | | |
| WT | B | — | 0.54 | — | 0.47 | |
| pH 7.5 | C | — | — | 0.39 | 0.47 | 0.44 |
| | | A | B | C | A | B |
| | | F7L | | | WT | pH 7.5 |

Fig. 6. R.m.s. differences (Å) compared for all atoms of the barnase F7L mutant and the wild-type pH 7.5 structures. The r.m.s. differences for each pair of molecules were calculated after least-squares superposition.

Table 4. *The interactions made by the side-chain of residue Leu7 in the F7L mutant structure*

| Residue in contact | Atom in contact | Distance (Å) | | |
|---|---|---|---|---|
| | | *A* chain | *B* chain | *C* chain |
| Ile88 | $C^{\delta 1}$ | 3.6 | 3.7 | 4.3 |
| Lys98* | $C^{\beta}$ | 4.1 | 3.7 | — |
| | $C^{\delta}$ | 3.5 | 3.3 | — |
| | $C^{\epsilon}$ | 4.0 | 4.2 | — |
| | $N^{\zeta}$ | 3.5 | 4.3 | — |
| Ile109 | $C^{\delta 1}$ | 3.5 | 3.4 | 3.4 |

* There is no data for residue Lys98 in the *C* chain because the side-chain atoms of this residue are disordered in the F7L mutant structure.

Table 5. *Local r.m.s. differences between atomic positions of the B chains of the F7L mutant and those of the wild-type* (pH 7.5) *structures*

| R.m.s. differences between F7L structure and wild-type pH 7.5 structure (Å) | | | | |
|---|---|---|---|---|
| Residue number | Main chain | Side chain | Water number | Deviation |
| Phe→Leu7 | 0.32 | – | Wat12 | Not found |
| Ile76 | 0.15 | 0.43 | Wat18 | 0.35 |
| Asn77 | 0.14 | 0.37 | Wat43 | 0.90 |
| Asp86 | 0.26 | 0.39 | Wat65 | New |
| Arg87 | 0.11 | 0.36 | | |
| Ile88 | 0.15 | 0.42 | | |
| Lys98 | 0.23 | 0.80 | | |
| Thr99 | 0.20 | 0.25 | | |
| Thr100 | 0.27 | 0.43 | | |
| Ile109 | 0.29 | 0.21 | | |
| Mean r.m.s. (Å) | 0.21 | 0.41 | Mean (Å) | 0.63 |

make new interactions with Leu7 in the F7L mutant (residues Ile88 and Ile109) have their atomic positions changed, within the limit of error (Table 5), with the exception of the side chain of Lys98. When all residues within 6 Å from the mutation site are considered, F7L has a localized mean r.m.s. deviation of 0.21 Å for main-chain atoms and 0.41 Å for side-chain atoms (Table 5), compared with the site in the wild-type structure. These local r.m.s. differences in atomic positions are considerably lower than those of the overall structure, revealing that the local structural changes are minimal.

The r.m.s. difference between the atomic positions of the side-chain of residue Lys98 in chain *B* of the wild-type and the F7L mutant is 0.80 Å. The side chain of Lys98 is displaced away from the site of mutation to avoid bad contact with the side chain of Leu7. This is the only significant structural relaxation observed concerning this mutation.

*Solvent structure at the mutation site*

The solvent-accessible surface area of Leu7 in the *B* chain is 35 $Å^2$ (20% exposed), that is a slight increase of 5 $Å^2$, comparing to residue Phe7 in the wild-type protein.

There are three water molecules that are close to the mutated side chain at residue 7, namely, Wat12, Wat18 and Wat43. These three waters are well conserved in position among the three chains of the mutant as well as among those of the wild type (Table 6), except that Wat43 is not found in wild-type chain *A* and Wat12 is not found in F7L chain *C*. The positions of all these waters deviate less than 1 Å from their equivalent positions in the wild-type structure. The water molecule Wat18 is observed in all chains of the wild type and all chains of the mutant. This water is well ordered ($B$ = 15 $Å^2$) and its position is well conserved with a deviation from its wild-type equivalent of 0.4 Å.

An additional fourth water molecule is observed near the mutation site in each of the three chains, but not in the same equivalent positions. Wat211 is found hydrogen bonded to the carbonyl O atom of residue Thr99, in both the *A* chain and the *C* chain. This water occupies a location very close to the hydrophobic 'pocket' generated by mutation and has a medium *B* factor ($\simeq$ 30 $Å^2$). This is to be compared with the mean *B* factor for the F7L protein

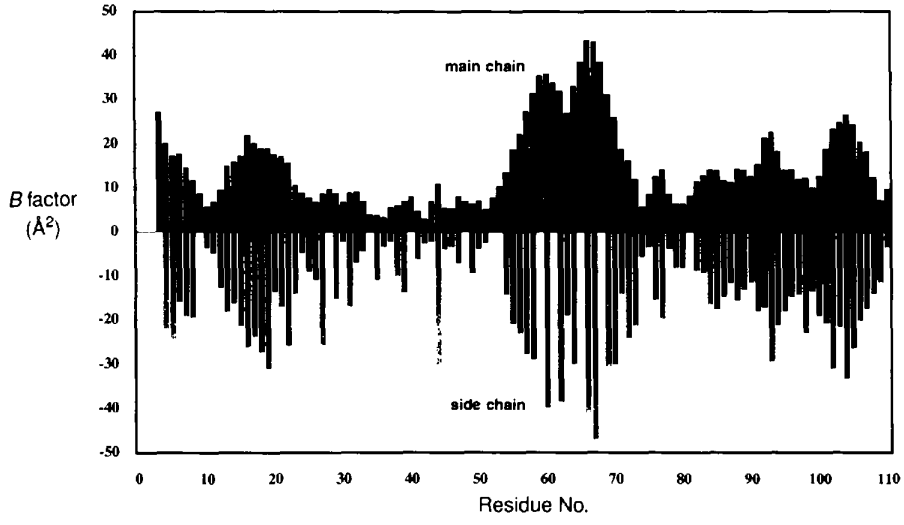


Fig. 7. Average temperature factors ($Å^2$) per residue for the F7L mutant chain *B*. Black lines are for the main-chain atoms, grey lines for side-chain atoms.

atoms of 16.6 Å$^2$ and that for the solvent molecules of 24.3 Å$^2$ (Table 3). The new water molecule found in chain *B* is hydrogen bonded to the N$^{\zeta}$ atom of Lys98 and it has a high *B* factor (43 Å$^2$).

*Conformation of the side chain of Leu7 compared with the rotamer library observations*

According to previous observations in well refined protein structures (Ponder & Richards, 1987), a leucine side chain in the hydrophobic core is likely to take up the conformation of either one of two rotamers. 64% of all leucines take up a conformation with $\chi_1$ close to –60° and $\chi_2$ close to 180°, while 25% take up one with $\chi_1$ close to 180° and $\chi_2$ close to +60°. Together, these two conformations account for 90% of all observed leucine side-chain conformations.

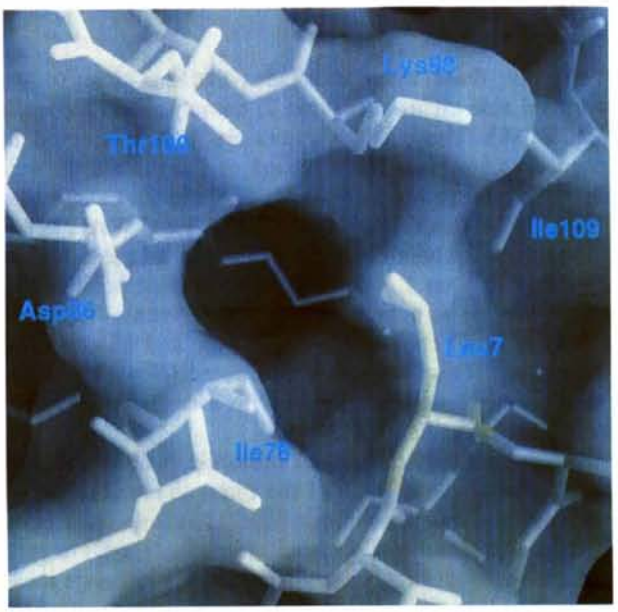


Fig. 8. The molecular surface of barnase F7L mutant showing the hydrophobic depression created on the surface of the protein by the mutation (the mutated residue, Leu7, is coloured yellow). The surfaces are colour coded according to surface curvature: the more concave, the darker grey. This figure is to be compared with Fig. 2 for the effect of the mutation.

Table 6. *Water molecules and their respective B factors found near the site of mutation in the F7L mutant and in the wild type*

The water chains *E*, *F* and *G* corresponds to the protein chains *A*, *B* and *C*, respectively. A missing value means that the corresponding solvent molecule is not found. Numbers in parentheses are the r.m.s. deviation (Å) of a mutant water from its equivalent position in the wild-type structure.

| | Hydrogen-bond partner(s) | Wild type pH 7.5 | | | F7L | | |
|---|---|---|---|---|---|---|---|
| | | *E* | *F* | *G* | *E* | *F* | *G* |
| Wat12 | Asp8 O$^{\gamma 2}$ Asp8 NH | 21.7 | 30.7 | 14.9 | 20.3 (0.47) | — | 25.9* (0.73) |
| Wat18 | Phe/Leu7 NH Asn77 O$^{\delta 1}$ | 18.6 | 12.0 | 25.3 | 15.0 (0.18) | 14.7 (0.35) | 40.0 (0.46) |
| Wat43 | Wat15 Wat51 Asp86 O$^{\delta 2}$ or Asn77 N$^{\delta 2}$ | — | 30.1 | 25.9 | 30.3 (—) | 31.2 (0.90) | 40.1 (0.60) |
| Wat211 (new) | Thr99 O | — | — | — | 33.2 | — | 26.7 |
| Wat65 (new) | Lys98 N$^{\zeta}$ | — | — | — | — | 43.0 | — |

* Disordered atom.

The side-chain torsion angles of the three chains of F7L are tabulated in Table 7. The torsion angles of Leu7 in chain *C* agree well with the second-most frequently observed rotamer conformation. Leu7 in chains *A* and *B* have $\chi_1$ angles close to the second-most preferred conformation while $\chi_2$ angles do not agree. This finding is surprising because it was expected that the Leu7 side chain will take up the best rotamer conformation when the mutant was first designed. When residue Phe7 of the wild-type structure was theoretically replaced with a leucine and this 'mutant' structure displayed with computer graphics, the side chain with the most frequently observed rotamer conformation appeared to reside quite happily in the cavity so created, without any severe bad contacts (Fig. 3).

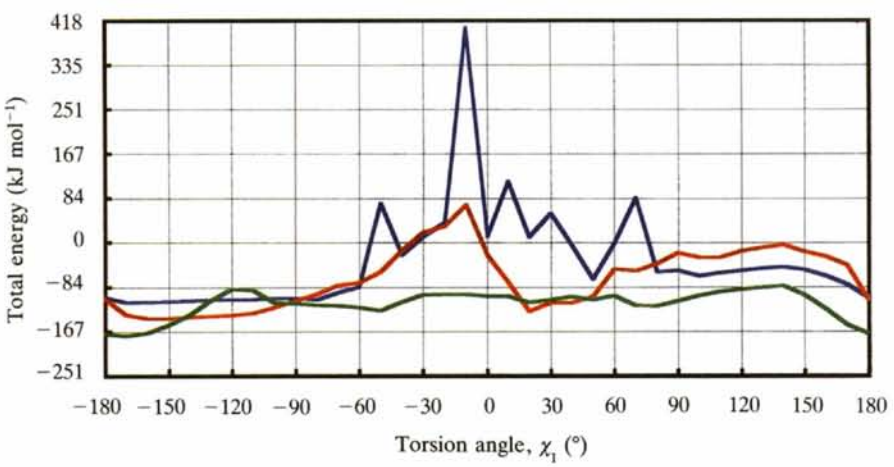


Fig. 9. Total energy *versus* torsion angle $\chi_1$ calculated for individual chains (blue for *A*, red for *B* and green for *C*) of the F7L mutant. The total energy was calculated with *X-PLOR* as the sum of the individual components: bond, angle, dihedral, improper, van der Waals and electrostatic.

Table 7. *Backbone and side-chain torsion angles of residue Leu7 of the barnase F7L mutant*

| | *A* | *B* | *C* |
|---|---|---|---|
| $\varphi$ | −53 | −51 | −45 |
| $\psi$ | −58 | −51 | −60 |
| $\chi_1$ | −159 | −138 | −168 |
| $\chi_2$ | 26 | 16 | 70 |

Notes: The side-chain angles from the backbone-independent rotamer library of Ponder & Richards (1987) for the best leucine rotamer are $\chi_1 = -64.9°$, $\chi_2 = 176.0°$; and those for the second best rotamer are $\chi_1 = -176.4°$, $\chi_2 = 63.1°$, with standard deviations in the range of 8 to 10°. The side-chain angles from the backbone-dependent rotamer library of Dunbrack & Karplus (1993) for the best leucine rotamer (with both $\varphi$ and $\psi$ in the range −40° to −60°) are $\chi_1 = 180° (\pm 60°)$ and $\chi_2 = 0°$ to 120°; and those for the second best rotamer are $\chi_1 = -60° (\pm 60°)$ and $\chi_2 = 120°$ to −120°. That is, the best backbone-independent rotamer corresponds to the second-best backbone-dependent rotamer, and *vice versa*.

A more recent study on side-chain rotamer configurations showed that there are significant correlations between side-chain torsion-angle probabilities and backbone $\varphi,\psi$ angles (Dunbrack & Karplus, 1993). This work led to a more elaborate 'backbone-dependent rotamer library' that is a refined and expanded version of the original one. The backbone torsion angles of residue Leu7 (Table 7) in F7L indicate that this residue belongs to the sub-class having both $\varphi,\psi$ ranging from –60° to –40°. Under this sub-class, the majority (56%) of leucine residues have $\chi_1$ equal to 180° (±60°) and 44% have $\chi_1$ = –60° (±60°). The order of the most frequently observed and the second-most frequently observed $\chi_1$ torsion angles are reversed when compared to the 'backbone-independent' rotamer library of Ponder & Richards (1987). Our experimentally obtained $\chi_1$'s agree with the observations in this new backbone-dependent rotamer library. The torsion angle $\chi_2$ of Leu7 also falls into the most frequently observed sub-division (46%), ranging from 0° to 120°.

*Conformation of the side chain of Leu7 studied by energy calculations*

Solving the crystal structure of the mutant does not give us an immediate explanation why the side chain of Leu7 takes up its observed conformation. Both model-F7L-1 and model-F7L-2 do not have obvious bad van der Waals contacts with their respective neighbouring residues. Energy calculations were performed to investigate whether there are other intrinsic features in the mutant structure that determine the Leu7 side-chain conformation. The calculations used here were based on the assumption that the major determinant of side-chain conformation of a leucine residue is its $\chi_1$ angle. The dependence of total and individual energy components on the $\chi_1$ angle were calculated for Leu7 in the F7L structure. The results of the total energy calculations were represented in Fig. 9. The variation in total energy is dominated by the van der Waals interaction energies and the conformational energy contributed by dihedral angles and bond angles (results not shown). The total energies calculated for individual chains of the F7L mutant have minima of 113, 142 and 175 kJ mol$^{-1}$(27, 34 and 42 kcal mol$^{-1}$) for chains *A*, *B* and *C*, respectively. The energy curve on chain *A* does not have a clear minimum but the lowest region corresponds to $\chi_1$ angles ranging from –150° to –170°. The energy curve for chain *B* has a lowest region corresponding to $\chi_1$ angles ranging from –140° to –160°. Total energy calculated for chain *C* shows a clear minimum at $\chi_1$ = –170°. Although the calculations for the *C* chain showed the best agreement with experimental results, one has to bear in mind that the *C* chain is the least reliable chain in this mutant. Taking it qualitatively, we see that the experimentally obtained $\chi_1$ angles fall within the range of calculated total energy minima, from –140° to –170°.

The total energies for the two modelled F7L mutants, derived from the wild-type structure, were also computed for comparison. Total energy calculated for individual chains of model-F7L-1 ($\chi_1$ = –60°) falls into the range from –155 to –192 kJ mol$^{-1}$ (–37 to –46 kcal mol$^{-1}$). Total energy calculated for individual chains of model-F7L-2 ($\chi_1$ = 180°) are –138 kJ mol$^{-1}$ (–33 kcal mol$^{-1}$) for both *A* and *B* chains and 6.3 kJ mol$^{-1}$ (+1.5 kcal mol$^{-1}$)

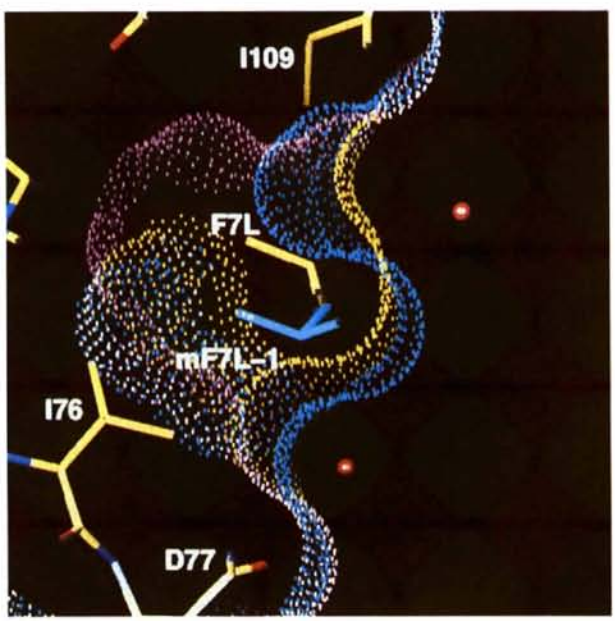


Fig. 10. A comparison of the hydrophobic surface areas buried by the side chain of Leu7 of two structures: yellow for the F7L crystal structure, and cyan for the model-F7L-1 structure. The magenta surface was calculated without residue 7 and represents the surface of the surrounding atoms before burial. The side chain of Leu7 in the F7L structure (yellow) buried a hydrophobic surface area of 45 Å$^2$ more than that of the model-F7L-1 structurte (cyan). The major difference is located in the space between the Leu7 side chain and the Ile109 side chain.

for *C* chain. The high energy in chain *C* is due to a poor van der Waals contact that cannot be relaxed by energy minimization. If we assume that the poor contact in chain *C* can be accommodated in some way and ignore the odd value for chain *C*, then all the energies calculated for all individual chains of both rotamers will be similar in magnitude and in the range −146 to −188 kJ mol$^{-1}$ (−35 to −45 kcal mol$^{-1}$). These values do not differ much from the minima derived from the crystal structure (the F7L '$\chi_1$-rotamers'). Taking the uncertainties and assumptions intrinsic in the calculations into consideration, the empirical energies calculated do not clearly discriminate one out of the two frequently observed side-chain conformations.

*Conformation of the side chain of Leu7 studied by molecular surface area calculations*

Burial of hydrophobic surface area away from the solvent has been considered to be a major driving force for the protein-folding event. This is mainly an entropic phenomenon which can be extended to the study of the side-chain conformation of Leu7 of the F7L mutant.

The surface area that is buried by residue Leu7 in each of the three structures, F7L, model-F7L-1 and model-F7L-2 are calculated (Table 8). There is good agreement between data of the *A* and *B* chains. The buried areas in F7L and its close relative, model-F7L-2 are similar and in the range 85 to 107 Å$^2$. In contrast, the buried area in the model-F7L-1 is only 41 to 49 Å$^2$. Therefore, the Leu7 residue in the F7L crystal structure buries as much as 45 to 50 Å$^2$ more than that buried by the same residue in the model-F7L-1 mutant (Fig. 10). The data extracted from the *C* chain is less reliable but it still indicates a difference of 23 Å$^2$. According to these calculations, the side-chain conformation of Leu7 in the F7L crystal structure is largely determined by how much surface area it can bury, in addition to energetic requirements.

Table 8. *Surface areas* (Å$^2$) *buried by the presence of residue* 7 *in the two modelled F7L rotamers compared to those of the crystal structure of F7L, calculated with the program MS* (*Connolly*, 1983)

| | *A* | *B* | *C* |
|---|---|---|---|
| Model-F7L-1 ($\chi_1 = -60°$) | 41 | 49 | 32 |
| Model-F7L-2 ($\chi_1 = 180°$) | 93 | 107 | 84 |
| F7L mutant | 85 | 98 | 55 |
| Difference between crystal structure and model-F7L-1 | 44 | 49 | 23 |

## Discussion

*Protein stability affected by mutation*

Systematic mutational analysis in our laboratory has established that the solvent-inaccessible side chain of Phe7 makes hydrophobic interactions and contributes 17 kJ mol$^{-1}$ (4.1 kcal mol$^{-1}$) to protein stability (Kellis, Nyberg, Sali & Fersht, 1988). The free-energy change of a Phe→Leu mutation estimated from free energies of transfer of amino acids from octanol to water (Fauchere & Pliska, 1983) is 0.54 to 0.59 kJ mol$^{-1}$ (0.13 to 0.14 kcal mol$^{-1}$), with or without correction for solute volume (Sharp, Nicholls, Friedman & Honig, 1991). This number is very small because both the volume and hydrophobicity of phenylalanine and leucine are very similar, and that is why the replacement of one by another is considered to be conservative. Our results showed that the environment in which the F7L mutation occurs is far from similar to the simplified picture of protein interior being modelled by small hydrocarbons. From our crystal structure of the F7L mutant, the mutated residue is on the surface and is partially accessible (20%) to solvent. The site is, therefore, heterogeneous with some parts being water-like and some parts being non-polar hydrocarbon like. Therefore, we need a more refined model to describe the free-energy change due to mutation.

The current model of estimating the energetics of a hydrophobic replacement mutation can be summarized by the equation (Sandberg & Terwillinger, 1991; Eriksson, Baase & Matthews, 1993),

$$\Delta\Delta G_{X\rightarrow Y} = \Delta\Delta G_{tr(X\rightarrow Y)} + \Delta\Delta G_{a/v(X\rightarrow Y)} + \Delta\Delta G_{site(X\rightarrow Y)}$$

where the free energy change ($\Delta\Delta G_{X\rightarrow Y}$) on mutating a hydrophobic residue *X* to another, *Y* is described by three terms: (1) the difference mutation energy [$\Delta\Delta G_{tr(X\rightarrow Y)}$] estimated by the free energies of transfer of the respective amino acids, *X* and *Y*, from an apolar solvent (*e.g.* octanol) to water; (2) a site-independent stabilization or destabilization term [$\Delta\Delta G_{a/v(X\rightarrow Y)}$] due to the change in area or volume on mutating *X* to *Y*; and (3) a site-specific interior packing energy term [$\Delta\Delta G_{site(X\rightarrow Y)}$] representing all other energies involved in mutating *X* to *Y*, such as geometric strains and differences in side-chain conformational entropy.

For the F7L mutant, a large part of destabilization can be accounted for by the second and third terms of the above equation. Since the mutation site is not completely buried and no enclosed cavity is created, the area/volume-dependent energy term will be estimated from area changes. From the F7L mutant structure, a large hydrophobic patch (50 Å$^2$) is exposed to the solvent. Our previous experiments have measured that in the major hydrophobic core of barnase, where wild-type Phe7 resides, the free energy change with respect to increase in core cavity area is 210 to 250 J mol$^{-1}$ Å$^{-2}$ (50 to 60 cal mol$^{-1}$ Å$^{-2}$) (Kellis, Nyberg & Fersht, 1989). Here we used the value of 210 J mol$^{-1}$ Å$^{-2}$ (50 cal mol$^{-1}$ Å$^{-2}$) (Sharp, Nicholls, Fine & Honig, 1991; Sharp, Nicholls, Friedman & Honig, 1991) to estimate the loss of free energy on creating such a surface. This accounts for 10.5 kJ mol$^{-1}$ (2.5 kcal mol$^{-1}$) of destabilization. The re-

maining 6.3 kJ mol$^{-1}$ (1.5 kcal mol$^{-1}$) of destabilization can be accounted for by the site-dependent packing free energy changes. It has been well established that protein interiors are highly heterogeneous, and the free energy contributed by the interior-packing effect is variable from site to site (Sandberg & Terwilliger, 1989; Sandberg & Terwilliger, 1991; Buckle, Henrick & Fersht, 1993; Eriksson, Baase & Matthews, 1993). From the crystal structure of F7L, this packing energy is mainly the result of losing extensive van der Waals interactions residue Phe7 makes with its neighbours, and the slight strain introduced by imperfect geometry of the side chain of Leu7. The pocket is not filled in by relaxation of the surrounding protein atoms, despite that the site is on the surface and the surrounding structure is relatively flexible. The lack of repacking and the existence of such a hydrophobic pocket in a protein is energetically unfavourable as their surrounding residues are located in a more densely packed environment. A small contribution of destabilization is also expected by mutating a weakly polar side chain (phenylalanine) to a non-polar side chain (leucine), because the polarity of the aromatic ring of phenylalanine can make favourable polar contact with the main-chain atoms of the protein interior (Sandberg & Terwilliger, 1991).

*Folding kinetics*

While the residue Phe7 is apparently not important for the correct folding into the final three-dimensional structure, this residue could be essential for the folding kinetics of the enzyme.

The importance of this residue in the folding pathway can be implicated by $\varphi$-value studies (Fersht, Matouschek & Serrano, 1992), based on experimental results extracted from kinetic and stability measurements on the mutant protein.

A quantity representing the extent of formation of an interaction in the transition state of folding is defined as,

$$\varphi_{\ddagger} = 1 - \Delta\Delta G_{\ddagger - F}/\Delta\Delta G_{U - F},$$

where $\Delta\Delta G_{U-F}$ is the change in free energy of unfolding on mutagenesis, relative to the folded state and $\Delta\Delta G_{\ddagger - F}$ is the change in activation energy of unfolding on mutagenesis, relative to the folded state. Similarly, a quantity representing the extent of formation of an interaction in the intermediate state of folding is defined as,

$$\varphi_I = 1 - \Delta\Delta G_{I - F}/\Delta\Delta G_{U - F},$$

where $\Delta\Delta G_{I-F}$ is the change in the energy levels of the major intermediate of folding upon mutagenesis relative to the folded state. A value of $\varphi = 0$ implies that the local structure at the site of mutation is as unfolded in the transition state ($\varphi_{\ddagger}$) or intermediate ($\varphi_I$) as it is in the unfolded state. Conversely, $\varphi = 1$ shows that the structure at the site of mutation is as folded in the transition state or intermediate as it is in the folded state.

Although we have not measured the $\varphi$ values for this mutant, we do have data measured with structural probes close to and flanking this residue. From interpolation of the data obtained for the mutants T6A, V10T and V10A (Matouschek, Serrano & Fersht, 1992), we know that both $\varphi_I$ and $\varphi_{\ddagger}$ of F7L are approximately equal to 0.3, indicating that the interactions of interest in this region of the hydrophobic core are only partially formed in the intermediate and then maintained at this extent until after the transition state, and then completed quickly to form the fully folded state. Apparently, the importance of this residue is in the consolidation of the hydrophobic core and the burial of extensive hydrophobic side chains after the transition state has been reached.

*The Phe→Leu mutation: is it conservative?*

Mutation of phenylalanine into leucine has been considered to be conservative despite the change in configuration of the $C^{\gamma}$ atom, from $sp^2$ to $sp^3$. The effect of this mutation is the replacement of an aromatic and slightly polar side chain (phenylalanine) by an aliphatic and non-polar side chain (leucine) with similar hydrophobicity. If the phenylalanine side chain is buried, the replacement with a leucine side chain can leave behind a cavity having a size of approximately 55 Å$^3$ (three times the size of a methylene group). At the same time, the hydrophobic interactions contributed by the $C^{\varepsilon 1}$, $C^{\varepsilon 2}$ and $C^{\zeta}$ atoms of the phenylalanine side chain will be removed. It is presumed in general that the substitution will be achieved with minimal structural disturbance. The stereochemical rationale for such an assumption is that the side-chain atoms $C^{\delta 1}$ and $C^{\delta 2}$ of a leucine residue can occupy similar locations of the side-chain atoms $C^{\delta 1}$ and $C^{\delta 2}$ of the phenylalanine residue.

This mutation has been employed routinely as a conservative replacement of a phenylalanine residue of interest in functional and structural studies of a number of proteins, for instance, snake toxins (Pillet *et al.*, 1993), p21 (Reinstein, Schlichting, Frech, Goody & Wittinghofer, 1991), endonuclease V (Nickell & Lloyd, 1991), rho protein (Brennan & Platt, 1991), a subunit of tryptophan synthase (Chen, Rambo & Matthews, 1992) and single-stranded DNA-binding protein (Bayer, Fliess, Greipel, Urbanke & Maass, 1989). In other cases, a phenylalanine residue of one protein has been found to have a leucine counterpart in a homologous protein. Naturally, the Phe→Leu mutation was used to probe the functions of these phenylalanine and leucine residues in these homologous proteins. Examples include the studies of dihydrofolate reductase (Thillet, Absil, Stone & Pictet, 1988; Prendergast, Appleman, Delcamp, Blakley & Freisheim, 1989; Wagner, Thillet & Benkovic, 1992), cytochrome *c* (Rafferty *et al.*, 1990), cytochrome P450 (Lindberg & Negishi, 1989), the reaction centre of *R.*

*sphaeroides* (Murchison *et al.*, 1993), phosphoglycerate kinase (Joào, Taddei & Williams, 1992) and carbonic anhydrase III (LoGrasso *et al.*, 1991). In most of these studies, the overall structural changes as detected by NMR and circular dichroism spectroscopy are minimal (Bayer, Fliess, Greipel, Urbanke & Maass, 1989; Reinstein, Schlichting, Frech, Goody & Wittinghofer, 1991; Joào, Taddei & Williams, 1992; Pillet *et al.*, 1993). Our results that the overall structure of the F7L mutant does not change on mutation agree with these findings.

While the Phe→Leu mutation is in general non-disruptive as far as the global structure is concerned, its local effect has not been well addressed. There are only two published examples in which the structure of a Phe→Leu mutant was studied at high resolution. The F153L mutant of T4 lysozyme (Eriksson, Baase & Matthews, 1993) was found to have the structure which is closest to the wild type, compared to replacements with methionine, isoleucine, valine and alanine. Moderately large relaxation (0.6 to 0.8 Å) of neighbouring side-chain atoms was observed towards the mutation site. The side-chain conformation of Leu153 ($\chi_1 = -75°$, $\chi_2 = +168°$) agrees well with that of the most frequently observed 'backbone-independent' rotamer (Ponder & Richards, 1987). The side-chain atoms $C^{\delta 1}$ and $C^{\delta 2}$ of Leu153 occupy equivalent positions of the side-chain atoms $C^{\delta 1}$ and $C^{\delta 2}$ of Phe153 of wild-type lysozyme. In this case, leucine represents a good conservative replacement of the phenylalanine. The recently published crystal structure of the F120L mutant of the semisynthetic enzyme, RNase 1–118:111–124, again showed no overall changes (deMel *et al.*, 1994). However, local structural rearrangements as large as 2.3 Å were observed. The $C^{\beta}$ and $C^{\gamma}$ atoms of the mutated residue are displaced by 0.61 and 0.67 Å, respectively, from the corresponding atoms of the Phe120 side chain in the wild-type structure.

The side chain of Leu7 in the barnase F7L mutant has a slightly strained conformation that is close to the most frequently observed conformation of the backbone-dependent rotamer library (Dunbrack & Karplus, 1993). Based on a simplified model that this side-chain conformation is mainly dependent on the $\chi_1$ torsion angle, empirical energy calculations showed that an energetically favourable side-chain conformation can have $\chi_1$ in the range −140° to −170°, which is consistent with our experimental results. However, energy calculations performed on individual chains cannot explain why the observed conformation is preferred to another frequently observed conformation, because the energy difference between these two states is not large enough to discriminate between them. Apparently, the side-chain conformation of Leu7 is largely dependent on an entropic effect: the burial of hydrophobic surface areas. Calculations on the crystal structure of F7L and on a modelled mutant reveal that the side-chain of Leu7 buries approximately 45 Å$^2$ of surface area *more* than the modelled F7L second-best backbone-dependent rotamer. It is this difference that drives the side chain of Leu7 to take up its unique conformation in the mutant crystal structure.

YWC is supported by a Croucher Foundation Scholarship, the Overseas Research Student Award and Imperial Chemical Industries p.l.c. The authors would like to thank Dr M. Hirshberg for helpful discussions about conformational energies of the Leu7 side chain. We would also like to thank the Science and Engineering Research Council for allowing us to use the synchrotron radiation facilities at Daresbury Laboratory. The atomic coordinates and structure factors of the barnase F7L mutant have been deposited in the Brookhaven Protein Data Bank.*

* Atomic coordinates and structure factors have been deposited with the Protein Data Bank, Brookhaven National Laboratory (Reference: 1BRG, R1BRGSF). Free copies may be obtained through The Managing Editor, International Union of Crystallography, 5 Abbey Square, Chester CH1 2HU, England (Reference: AD007). A list of deposited data is given at the end of this issue.

## References


BAYER, I., FLIESS, A., GREIPEL, J., URBANKE, C. & MAASS, G. (1989). *Eur. J. Biochem.* **179**, 399–404.

BRENNAN, C. A. & PLATT, T. (1991). *J. Biol. Chem.* **266**, 17296–17305.

BRÜNGER, A. T., KURIYAN, J. & KARPLUS, M. (1987). *Science*, **235**, 458–460.

BUCKLE, A. M., HENRICK, K. & FERSHT, A. R. (1993). *J. Mol. Biol.* **234**, 847–860.

CAMERON, A. D. (1992). PhD thesis, Univ. of York, England.

CHEN, Y. W. (1994). PhD thesis, Univ. of Cambridge, England.

CHEN, Y. W., FERSHT, A. R. & HENRICK, K. (1993). *J. Mol. Biol.* **234**, 1158–1170.

CHEN, X., RAMBO, R. & MATTHEWS, C. R. (1992). *Biochemistry*, **31**, 2219–2223.

COLLABORATIVE COMPUTATIONAL PROJECT, NUMBER 4 (1994). *Acta Cryst.* D**50**, 760–763.

CONNOLLY, M. L. (1983). *Science*, **221**, 709–713.

DUNBRACK R. L. JR & KARPLUS, M. (1993). *J. Mol. Biol.* **230**, 543–574.

ERIKSSON, A. E., BAASE, W. A. & MATTHEWS, B. W. (1993). *J. Mol. Biol.* **229**, 747–769.

FAUCHERE, J.-L. & PLISKA, V. (1983). *Eur. J. Med. Chem. Chim. Ther.* **18**, 369–375.

FERSHT, A. R., MATOUSCHEK, A. & SERRANO, L. (1992). *J. Mol. Biol.* **224**, 771–782.

HENDRICKSON, W. A. (1985). *Methods Enzymol.* **115**, 252–270.

HILL, C. P. (1986). PhD thesis, Univ. of York, England.

JOÀO, H. C., TADDEI, N. & WILLIAMS, R. J. P. (1992). *Eur. J. Biochem.* **205**, 93–104.

JONES, T. A. & KJELDGAARD, M. (1993). *O*. Version 5.9. Uppsala Univ., Sweden.

JONES, T. A., ZOU, J. Y., COWAN, S. W. & KJELDGAARD, M. (1991). *Acta Cryst.* A**47**, 110–119.

KABSCH, W. & SANDER, C. (1983). *Biopolymers*, **22**, 2577–2637.

KELLIS, J. T. JR, NYBERG, K. & FERSHT, A. R. (1989). *Biochemistry*, **28**, 4914–4922.

KELLIS, J. T. JR, NYBERG, K., SALI, D. & FERSHT, A. R. (1988). *Nature (London)*, **333**, 784–786.

KRAULIS, P. (1991). *J. Appl. Cryst.* **24**, 946–950.

LINDBERG, R. L. P. & NEGISHI, M. (1989). *Nature (London)*, **339**, 632–634.

LoGrasso, P. V., Tu, C. K., Jewell, D. A., Wynns, G. C., Laipis, P. J. & Silverman, D. N. (1991). *Biochemistry*, **30**, 8463–8470.
Luzzati, V. (1952). *Acta Cryst.* **5**, 802–810.
Matouschek, A., Serrano, L. & Fersht, A. R. (1992). *J. Mol. Biol.* **224**, 819–835.
Mauguen, Y., Hartley, R. W., Dodson, E. J., Dodson, G. G., Bricogne, G., Chothia, C. & Jack, A. (1982). *Nature (London)*, **297**, 162–164.
deMel, V. S. J., Doscher, M. S., Glinn, M. A., Martin, P. D., Ram, M. L. & Edwards, B. F. P. (1994). *Protein Sci.* **3**, 39–50.
Murchison, H. A., Alden, R. G., Allen, J. P., Peloquin, J. M., Taguchi, A. K., Woodbury, N. W. & Williams, J. C. (1993). *Biochemistry*, **32**, 3498–3505.
Nicholls, A. (1992). *GRASP: Graphical Representation and Analysis of Surface Properties*. Version 1.04. Columbia Univ., New York, USA
Nickell, C. & Lloyd, R. S. (1991). *Biochemistry*, **30**, 8638-8648.
Pillet, L., Trémeau, O., Ducancel, F., Drevet, P., Zinn-Justin, S., Pinkasfeld, S., Boulain, J.-C. & Ménez, A. (1993). *J. Biol. Chem.* **268**, 909-916.
Ponder, J. W. & Richards, F. M. (1987). *J. Mol. Biol.* **193**, 775-791.
Prendergast, N. J., Appleman, J. R., Delcamp, T. J., Blakley, R. L. & Freisheim, J. H. (1989). *Biochemistry*, **28**, 4645–4650.
Rafferty, S. P., Pearce, L. L., Barker, P. D., Guillemette, J. G., Kay, C. M., Smith, M. & Mauk, A. G. (1990). *Biochemistry*, **29**, 9365–9369.
Reinstein, J., Schlichting, I., Frech, M., Goody, R. S. & Wittinghofer, A. (1991). *J. Biol. Chem.* **266**, 17700–17706.
Sandberg, W. S. & Terwilliger, T. C. (1989). *Science*, **245**, 54–57.
Sandberg, W. S. & Terwilliger, T. C. (1991*a*). *Proc. Natl Acad. Sci. USA*, **88**, 1706–1710.
Sandberg, W. S. & Terwillinger, T. C. (1991*b*). *Trends Biotechnol.* **9**, 59–63.
Sharp, K. A., Nicholls, A., Fine, R. F. & Honig, B. (1991). *Science*, **252**, 106–109.
Sharp, K. A., Nicholls, A., Friedman, R. & Honig, B. (1991). *Biochemistry*, **30**, 9686–9697.
Thillet, J., Absil, J., Stone, S. R. & Pictet, R. (1988). *J. Biol. Chem.* **263**, 12500–12508.
Wagner, C. R., Thillet, J. & Benkovic, S. J. (1992). *Biochemistry*, **31**, 7834–7840.